Laser beam welding of austenitic manganese-alloyed stainless steels

Soldagem a Laser de Aço Inoxidável Austenítico ao Manganês

M.Sc. V. Quiroz, Dr.-Ing. A. Gumenyuk and Univ.-Prof. Dr.-Ing. M. Rethmeier
BAM Federal Institute for Materials Research and Testing, Berlin, Germany

Abstract

Due to volatile nickel prices, high manganese alloys are currently being introduced as an alternative to conventional CrNi-stainless steels. In this study, fast and cost-effective laser beam welding of these steel grades has been investigated. A central aspect concerns hot crack formation which needs to be clarified in order to ensure the safety of the joined components. Comparative laser beam welding experiments on 1.5 mm to 3 mm thick sheets of austenitic CrMnNi-steels and standard austenitic steel grades have been performed using a CO_2-laser.

Sheet thickness in conjunction with the steel grade and welding parameters have proved to exert a major influence on the occurrence of internal imperfections, such as pores and cracks, especially for high manganese alloyed stainless steels. Though, both pore and crack formation can be prevented by adequate parameter settings.

Results of conducted Controlled Tensile Weldability (CTW) tests indicate a higher hot cracking susceptibility of the CrMnNi-steels, which is consistent with the phenomena observed in the experimental welds.

Resumo

Devido aos preços voláteis de níquel, ligas de alto teor de manganês estão atualmente sendo introduzidos como uma alternativa ao convencional aços inoxidável CrNi. Neste estudo de soldagem por feixe laser rápida e rentável destes aços tem sido investigada. Um aspecto central diz respeito à formação de trincas a quente, que deve ser esclarecido a fim de garantir a segurança dos componentes que se deseja unir. Os experimentos comparativos da soldagem por feixe laser de chapas de 1,5 mm a 3 mm de espessura de aços austeníticos CrMnNi e aços austeníticos padrão foram realizadas utilizando um laser de CO_2.

A espessura da chapa em conjunto com o tipo de aço e os parâmetros de soldagem exercem uma grande influência sobre a ocorrência de falhas internas, tais como poros e fissuras, especialmente em relação ao aço inoxidável de alto manganês. Embora, tanto os poros como a formação de trincas podem ser impedidas através da escolha de parâmetros de soldagem adequados.

Resultados de testes de "Controlled Tensile Weldability" (CTW) indicam uma maior susceptibilidade à fratura a quente do aço CrMnNi, que é consistente com os fenômenos observados nas soldas experimentais.

Introduction

Laser beam welding offers many advantages in industrial processing in comparison to other welding processes and finds several applications e.g. in automotive construction or in tube profile fabrication [8]. The main advantage of the laser beam welding process concerns the concentrated, but low heat input into the specimen, allowing high welding speeds to be reached. Specially, regarding austenitic stainless steels, this leads to low distortions in the welded structures, despite of their high thermal expansion coefficient and low thermal conductivity. Furthermore, the thermal input and the high processing speeds reduce metallurgical damage, as the formation of chromium carbides, which have a detrimental effect on corrosion resistance, can be hindered.

In austenitic manganese-alloyed stainless steels, nickel which is normally the most expensive constituent of the material is partly replaced by lower-cost manganese and smaller amounts of nitrogen. These steels offer a cost-effective alternative to conventional CrNi- stainless steels in view

of the instabilities in the nickel price seen during the last years. Analysis of the raw material cost evolution reveals a continuous increase of the primary nickel price since the end of 2008 (after a sharp decline during the year 2007) from 9000 US$/T to actually 26 000 US$/T (according to the London Metal Exchange LME).

Concerning the properties of Mn-austenitic steels, it can be remarked that although manganese is a weak austenite former, it increases the solubility of nitrogen which is a strong austenite former [21] and enhances the mechanical strength of the material. This results into a wide scope for new weight reduction applications. Furthermore, the instability of the austenitic microstructure tends to cause a strong work hardening effect which involves a high capacity for crash energy absorption. To reduce work hardening and improve deep drawing properties copper can be added [3, 8]. Copper and nitrogen have also been identified to upgrade corrosion resistance [19, 20].

As the wide application of these materials depends on the joining characteristics, weldability needs to be investigated. However, there are up to the present only a limited number of research studies relating to this aspect.

The limitations of the laser process for welding alloys containing volatile elements like manganese were studied in [14]. Factors affecting alloying element vaporization from laser-melted pools in high-manganese stainless steels were presented. Manganese loss by laser beam welding of stainless steels of the 200 series, using a subkilowatt CO_2 laser, caused changes in the chemical composition of the material and was attributed to a small weld pool size and high laser powers. In [2], eruptions in the weld that result in excessive weld spatter, concavity and porosity were reported during electron beam welding of high Mn, high N austenitic stainless steels. It was concluded that the weld quality is extremely parameter dependant and not reproducible.

The impact of the energy input by TIG, GMA and laser beam welding on the weld quality and mechanical strength of the cold-worked steel grades 1.4376 (CrMnNi-steel) and 1.4301 (CrNi-steel) was studied, although not extensively in [11]. It was stated that laser welds of 1.4376 obtained the highest yield strength. Also hot crack susceptibility was examined in [11] for welds produced by TIG-welding with the programmable deformation crack (PVR) test. In this test, tensile strain is linearly increased during welding. Hot cracking resistance of 1.4376 was found to be slightly better than that of 1.4301.

Regarding hot crack formation by laser beam welding, former and ongoing research at BAM has identified that centreline solidification cracks can occur in manganese alloyed stainless steels under certain welding conditions, whereas standard CrNi-steels remain defect free.

In this study, laser weldability of two austenitic manganese-alloyed stainless steels (1.4371 and 1.4376) in comparison to conventional CrNi-steels (1.4301 and 1.4318) will be discussed. The aim is to find adequate welding process windows and conditions for avoiding hot crack formation. Information regarding possible manganese losses will be gained with the help of electron probe X-ray micro-analysis (EPMA) measurements. Electron backscatter diffraction (EBSD) investigations will provide information about the base material and weld metal microstructure that is not possible to obtain by conventional metallographic inspections. Hot cracking susceptibility will be investigated by means of the CTW-Test. The influence of the applied strain rate on hot crack formation, in terms of the resulting crack length, will be examined in dependence of the steel grade and compared with obtained experimental welding results for validation.

Materials and Methods

The materials used in this investigation were the manganese alloyed stainless steels 1.4371 (AISI 201L) and 1.4376 (Nirosta® H400) with a thickness of 3.2 mm and 1.5 mm, respectively. For comparative welding experiments the conventional austenitic steels 1.4301 (Nirosta® 4301) and 1.4318 (AISI 301L) were selected. The material composition and thickness is presented in Table 1.

Table 1: Compositional analysis of the investigated materials (mass %)

Steel	d in mm	C	Cr	Ni	Mn	Si	P	S	Cu	Nb	Mo	N	Fe
1.4318	3.2	0.02	17.61	7.51	1.09	0.52	0.026	0.002	0.18	0.02	0.17	0.09	Bal.
1.4371	3.2	0.03	16.77	4.86	7.13	0.40	0.026	0.006	0.34	0.02	0.10	0.13	Bal.
1.4301	1.5	0.04	18.82	8.79	1.36	0.38	0.027	0.004	0.45	0.01	0.19	0.05	Bal.
1.4376	1.5	0.03	18.03	5.09	6.55	0.42	0.023	0.005	0.23	0.01	0.10	0.15	Bal.

Both 3.2 mm sheets 1.4371 and 1.4318 were delivered in the cold rolled condition. Alloys 201L and 301L are the lower carbon versions of 201 and 301, respectively. Stainless steel grade 301L is a slightly lower alloy (lower cost) replacement for 1.4301. The mechanical properties of the studied alloys are presented in Table 2.

Table 2: Mechanical properties of the materials

	1.4318	1.4371	1.4376	1.4301
$R_{p0,2}$ in MPa	570	715	400	300
R_m in MPa	860	920	750	650
$A_{50\ mm}$ in %	40	35	50	55

Welding experiments were performed using a CO_2 laser (Fig. 1**,** left), delivering an effective output of up to 5 kW and with a 200 mm focal distance.
Bead-on-plate, butt and overlap welds were produced with different welding parameters by changing the heat input and welding speed. The focal point position was additionally varied for a set of bead-on-plate welding experiments. For butt joints, laser cutting was employed for weld edge preparation. Argon was used as forming gas. As shielding gas a mixture of helium and argon (50/50) was applied coaxially.
The CTW-Test (Fig. 1, right) was used in conjunction with CO_2 laser keyhole welding to investigate hot cracking susceptibility of both 3.2 mm thick sheets of the steel grades 1.4371 and 1.4318. This test allows the application of tensile strain at a variable fixed cross-head speed transverse to the welding direction.
For the experiments test coupons (150 mm x 30 mm x 3.2 mm) were arc welded to the clamping adaptors (150 mm x 250 mm x 8 mm) of the CTW- test facility.

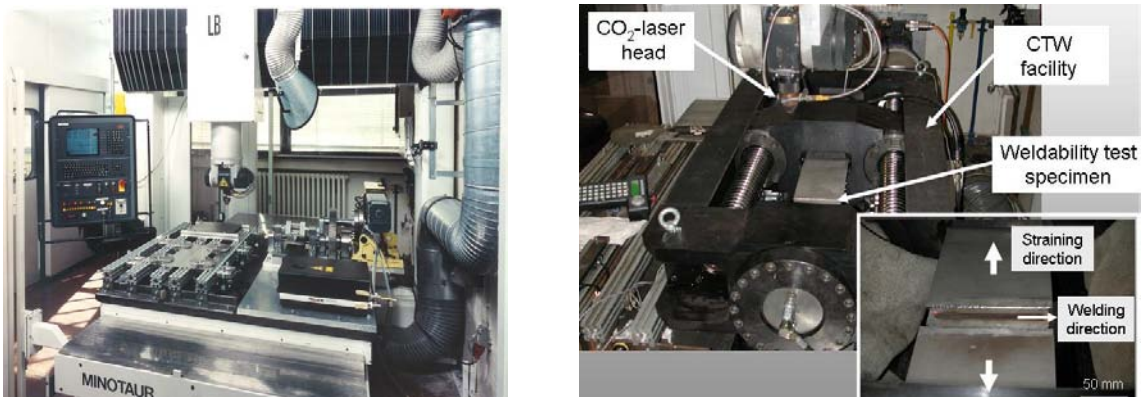

Fig. 1: Experimental set-up, CO_2-laser equipment (left) and CTW-Test facility (right)

Standard metallographic techniques were used for microstructural analysis. Complementary investigations relating to phase transformation were conducted with the ESBD technique. Vickers microhardness was determined at a load of 0.5 kg. Furthermore, the obtained welds were subjected to radiographic tests for detection of internal imperfections. The effect of the welding parameters on the vaporization and loss of manganese was investigated by EPMA with a JEOL-microprobe JXA-8900 RL.

Results

Bead-on-plate welds

Bead-on-plate welds were carried out to analyze the influences of the process parameters on the weld quality. Full 3^2 factorial experiments were performed varying the laser power P_L and welding speed v, according to the sheet thickness d, and maintaining the focal point position F constant (Table 3).

Table 3: Parameters for full 3^2 factorial bead-on-plate welding experiments

d in mm	levels	Factors		
		P_L in kW	v in m/min	F in mm
1.5	1	2.4	6	0
	2	3.6	8	
	3	5	10	
3.2	1	2.4	5	-1
	2	3.6	6	0, -1, -1.8
	3	5	7	-1

The welding speed and focal point position were found to have a significant effect on weld pool stability and spatter formation only on the high manganese stainless steels. Specially, the steel grade 1.4371 (with d=3.2 mm) shows a remarkable tendency to spatter formation at a moderate travel speed (v=5 m/min) and laser power (P_L=3.6 kW) when the laser beam is focused 1 mm below the surface. By increasing or decreasing the focal point position to -1 mm or -1.8 mm, respectively, spatter formation can be reduced. The resulting penetration depth t and weld form may play a major role in the unstable behaviour of the weld cavity. Shallow welds (with t equal to approx. one half of the sheet thickness) exhibited a satisfactory surface appearance. At deeper penetrations, the cavity formed during laser beam welding can become unstable in case of the high manganese alloyed steels, and spatter arises. Though, spattering can be avoided by accurate parameter settings, e.g. by increasing the welding speed or varying the focal point position, as noted above.

Butt and lap welded joints

To produce butt and lap welds at different sheet thicknesses, the laser power was varied in the range between 2.4 kW and 5 kW and the welding speed was accordingly adjusted (Table 4).
A stable welding process was achieved for all butt and lap joints at the selected welding parameters.

Table 4: Experimental welding parameters

d in mm	Parameter for butt welded joints			Parameter for lap welded joints		
	P_L in kW	v in m/min	F in mm	P_L in kW	v in m/min	F in mm
1.5	2.4	3	0	2.4	2.5	0
	3.6	4		3.6	3	
	5	6		5	6	
3.2	2.4	1.5	-1	2.4	0.5, 1	-2
	3.6	2		3.6	1, 1.5, 2	
	5	3		5	1.8, 2, 2.5, 3	

For all butt welding experiments, the obtained weld quality meets the requirements of the highest assessment group B in EN ISO 13919-1.

Minor spatter formation is observed by laser beam welding of both 1.5 mm sheets (1.4376 and 1.4301) in the lap joint configuration. Though a stable process, good weld appearance and inner quality (group B, according EN ISO 13919-1) can be reached.

Regarding the 3.2 mm sheets, the obtained weld appearance can also be classified into group B. But considering the high penetration depth and the lap joint configuration, avoiding pore formation becomes problematic.

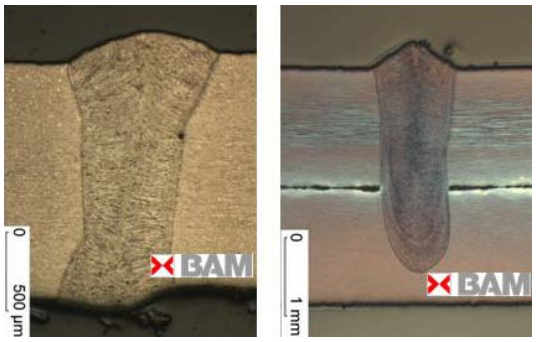

Fig. 2: Butt and overlap weld (1.4376)

As shown in Fig. 3, porosity proves to be strongly parameter dependent. At low laser powers and with increasing penetration depth, pore formation is more intense and not acceptable. In addition, crack occurrence is observed at the highest investigated laser power and resulting penetration depths for the manganese alloyed steel 1.4371. Such cracks originate inside the weld and can only be detected from radiographic films.

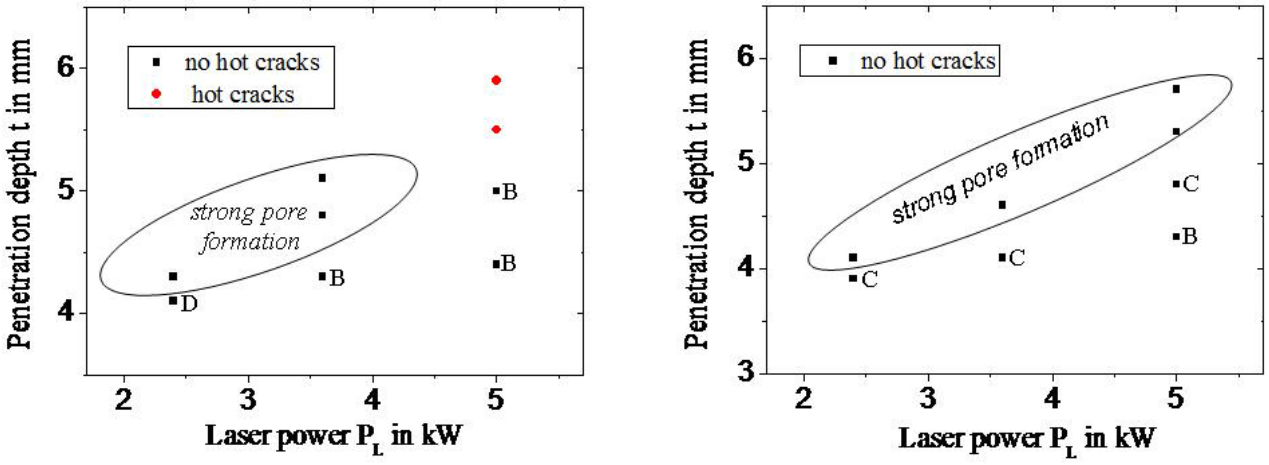

Fig. 3: Process windows for 3.2 mm lap welded joints of the materials 1.4371 (left) and 1.4318 (right). Evaluation of internal imperfections, regarding hot crack occurrence and classification of porosity into groups (B-D), according EN ISO 13919-1

SEM examinations revealed smooth dendritic features on the surface of the formed cracks (Fig. 4), which are similar to those found in solidification crack surfaces. Furthermore, it is observed that the contours of the solidification fronts fit together. This provides evidence of centreline solidification crack formation in the test welds. Such cracks are believed to occur in the last stages of solidification by separation of grains or dendrites due to the rupture of liquid films, caused by thermal and mechanical strains. Their formation is complex in nature and involves an interaction between metallurgical, process and design influencing variables.

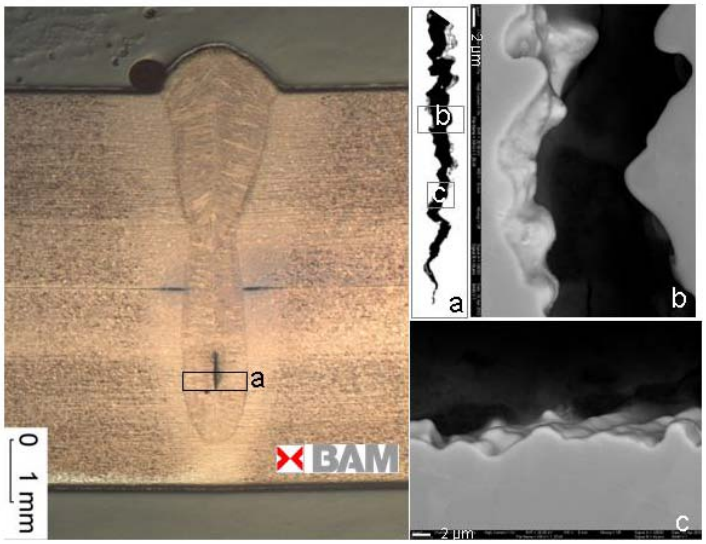

Fig. 4: Cross section (left) of overlap weld (1,4372, P_L=5 kW, v=2 m/min, F=0) and SEM image of the crack surface (right)

Microstructure

All base materials exhibit an austenitic structure which contains only small amounts of delta ferrite. Ferritescope measurements determined a 0.2% rest ferrite content in the 1.5 mm sheets. Cold rolled 3.2 mm materials (Fig. 5, a) were found to have a higher content of magnetic constituents, i.e. approx. 1 %. EBSD examinations performed for these materials show that apart from a large amount of stacking faults, high density dislocations and twin crystals, strain induced martensite with a BCC structure (Fig. 5, b) formed as product of the underwent deformation, being this tendency more pronounced in case of the material 1.4371. SEM examinations captured a small amount of precipitations in the manganese alloyed steel 1.4371, which were identified as MnS by means of EDX analysis. From cross sections of the base material 1.4376, precipitations are visible and can be identified as CrN_2, according to [15].

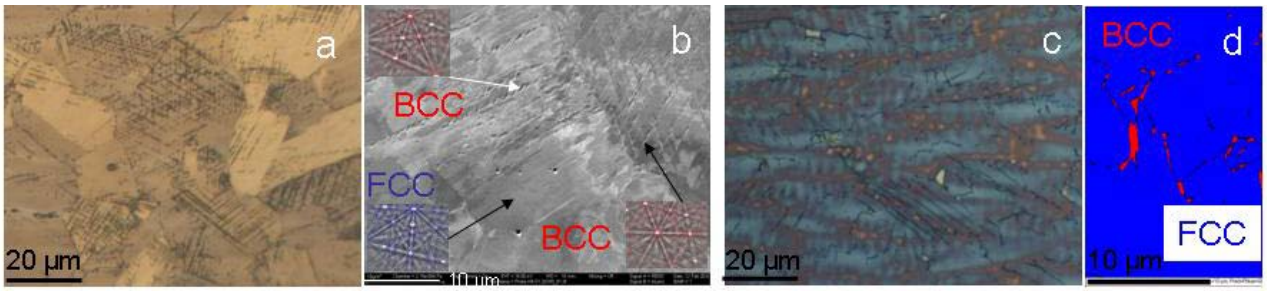

Fig. 5: Micrographs of 1.4371 showing the base material structure (a) and weld metal microstructure (c). EBSD measurements in the base material (b) and weld metal (d) distinguish and identify FCC and BCC structures

The microstructure of the weld metal consists of austenite and a small quantity of δ-ferrite, retained at the dendrite cores (Fig. 5, c and d). This is a proof of ferritic-austenitic solidification. It must also be remarked that at high cooling rates, typical for laser beam welding, the amount of δ-ferrite tends to increase and can not be further determined by magnetic measurements due to the small dimensions of the weld. Estimation of the ferrite content from micrographs by image analysis software is difficult, if not impossible, because ferrite is finely distributed within dendrites (Fig. **5**, c). With the EBSD technique, detection of δ-ferrite can be accomplished (Fig. 5, d) and also quantified, though only in limited regions, due to the required high magnifications (x 10 000). Metallographic examinations indicate that by the manganese alloyed steels, the tendency to retain ferrite is higher, in accordance to [11]. Chromium carbide precipitation does not occur during the welding process, due to the rapid heating and cooling during laser beam welding. Microstructural changes are noted in the heat affected zone (HAZ) of the cold rolled materials. Dislocation density diminished and martensite transformed into austenite, as consequence of the experienced welding thermal cycle. This is reflected in the hardness measurement results, where a continuous decrease of the hardness values from 280 HV0.5 in the base material to ca. 240 HV0.5 in the HAZ and in the weld metal is observed. Both 1.5 mm sheets (1.4376 and 1.4371) show comparable values of around 200 HV 0.5 in the base material, heat affected zone and weld metal.

The primary solidification mode can be best described using Hull´s and Hammer and Svenson´s Cr/Ni-equivalents, where the FA modus: $L \rightarrow L+\delta \rightarrow L+\delta+\gamma \rightarrow \delta+\gamma$ is predicted. Moreover, ferrite numbers of about 0-5% and 5-10% can be estimated from H&S and Hull diagrams respectively.

EPMA results

Serial analyses were performed for bead-on-plate, butt and lap welds to gain information about the potential loss of manganese, which has a lower enthalpy of evaporation than iron, in the welded structure (Table 5).

Table 5: Average, min. and max. measured manganese concentration in weight-% for bead-on-plate, butt and lap welds

Condition	Base material	Bead-on-plate 3.6 kW, 5 m/min	Butt welded joint 5kW, 6 m/min	Lap welded joint 5 kW, 2 m/min	
		Weld metal	Weld metal	Weld metal	
				top	bottom
Mn - Average	7.1	7.1	6.6	7.0	6.9
Mn - Minimum	6.6	6.2	6.1	6.4	6.7
Mn - Maximum	8.0	7.6	7.3	7.4	7.2

Regarding the bead-on-plate weld produced at 3.6 kW and 5 m/min, which exhibited severe spattering, variation of the manganese content in the weld metal, in comparison to the base material can not be observed. This indicates that spatter formation is not necessarily accompanied by intense expelling of vaporized elements.
Manganese loss during laser beam welding in the butt joint configuration, which may favour degassing of vaporized metal, is not very significant. Only a decrease in weld metal manganese content of approx. 7% was detected. From micrographs, microstructural changes relative to the butt and lap weld samples could not be noticed. It must also be considered that the average value lies within the measured concentration range of the base material and of the other welds.
In the examined lap weld, no differences in manganese content in the upper and lower weld part (where a crack was located (Fig. 4)) were detected. This suggests that, at high penetration depths emerging pores may be trapped between converging dendrites during solidification.

Hot cracking susceptibility - CTW-Test
Full penetration bead-on-plate welds of 125 mm length were produced with a high energy input (5 kW, 1.5 m/min) at a focal point position of -1 mm by applying 50/50 He/Ar as shielding gas. Tests were run at different cross-head-speeds, thus altering strain conditions during welding which are believed to influence the hot crack susceptibility of the materials.

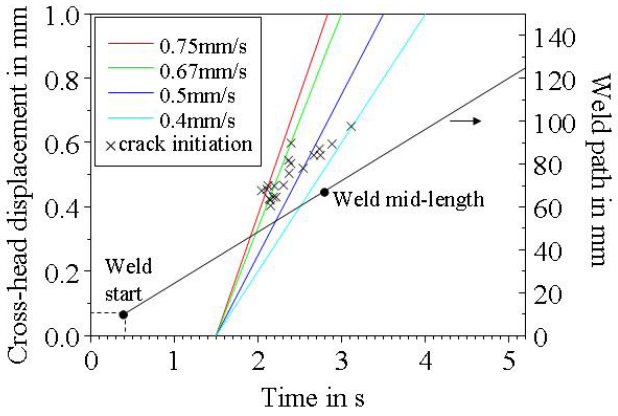

Fig. 6: Diagram showing the CTW-Test procedure (including the weld path and strain application) and position of crack initiation for both investigated materials

The CrMnNi-steel 1.4371 and the standard CrNi-steel 1.4378 were selected for the experiments. Test conditions included the application of a pre-load of 2 kN, weld start at 10 mm distance from the plate edge, strain application at 32.5 mm distance from the weld start location and limitation of the cross-head travel to 1mm (limiting the maximum load to below 180kN). Fig. 6 gives an insight into the CTW-Test procedure, which includes the weld path, applied strains and the position of resulting hot cracks.

The cross-head speed was increased from 0.4 mm/s, at which the reference material 1.4318 did not show any cracking, to 0.75 mm/s. Crack formation was analysed in dependence of the applied deformation and the steel grade taking account of the resulting overall crack length.

Hot cracks do not occur on the sample surface, but deeper inside the weld metal. Therefore, information about the crack position and length was obtained from radiographic films. It can be observed that continuous cracks form in the weld centreline (Fig. 7). In some cases, more cracks (up to two) were found per sample. From Fig. 6 , it is visible that crack formation occurs in the proximity of the weld mid-length. The cack initiation position depends on the applied cross-head speed. Hot cracks were found between ca. 10 mm (at the highest deformation rate) to ca. 60mm (at the lowest deformation rate) beyond the point where strain was first applied.

Fig. 7: Radiographic film showing a weld centreline crack in the material 1.4371, tested at a cross-head speed of 0.6 mm/s

The CTW-Test results show a higher hot cracking susceptibility of the manganese alloyed stainless steel 1.4371. This is reflected in the resulting higher overall crack length in comparison to the standard CrNi-steel 1.4318 at all investigated cross-head speeds (Fig. 8). Furthermore, no distinct boundary between crack and no-crack formation can be observed for the steel grade 1.4318. This phenomenon still needs to be examined.

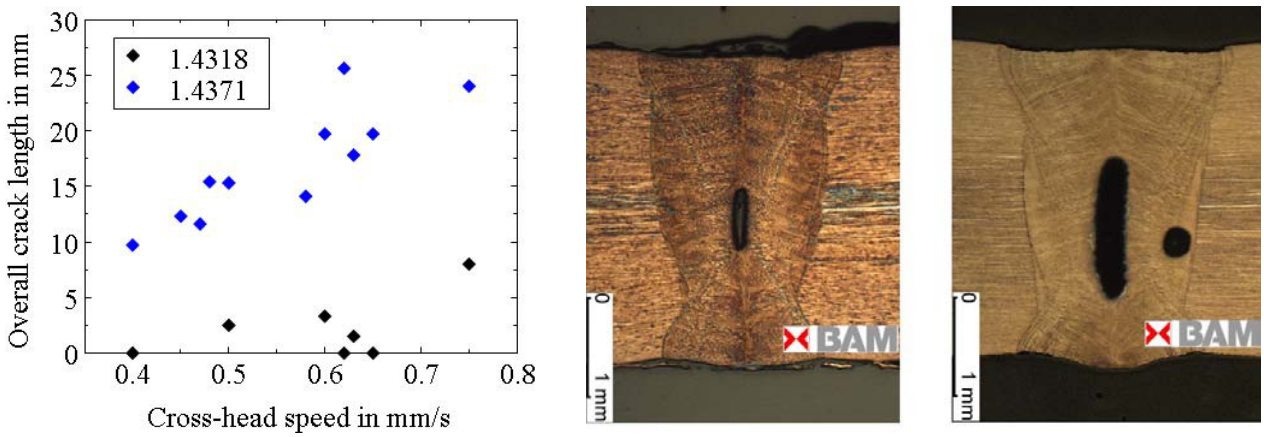

Fig. 8: CTW-Test results showing the resulting overall crack length in dependence of the applied cross-head speed and steel grade (left). Cross sections of welds produced with the CTW-Test at a cross head-speed of 0.63 mm/s (right)

Hot crack dimensions are not comparable between the two investigated materials as shown in Fig. 8 (right). Hot cracks found in the CrMnNi-steel 1.4371 are not only longer, but also much wider and larger in the vertical direction. This is also indicative of the higher hot cracking susceptibility of this material in comparison to the CrNi-steel 1.4318. The inferior ductility properties (as presented in Table 2) may also have an influence on the resulting crack geometry, as the capability of the material to withstand deformation strains is correspondingly lower.

Discussion

Comparative welding experiments on standard and high-manganese alloyed stainless steels showed differences in weldability, regarding principally the welding process stability and hot crack susceptibility.

Considerable spatter formation was only observed in bead-on-plate welds of the high-manganese alloy steels under certain welding conditions (e.g. at the lowest investigated travel speeds) that probably led to weld instabilities. Degassing of the molten material may be involved in this process, as proposed in [2]. As the keyhole is formed, unstable behaviour can lead to collapse and cause void formation. It is believed that the vaporized metal is able to expand the created voids, inducing the expelling of the molten material. The welding speed has a significant effect on the keyhole stability. High speed video observations of the melt pool in [13] showed, that low welding speeds which result in a larger molten pool prevent spattering.

Furthermore, the relatively high vapour pressure of manganese compared with iron points to the potential problem of evaporative loss. It is believed that the change of the chemical composition of metal in the weld pool is controlled by the material evaporation from the keyhole surface and diffusion into the melt [9]. An important influencing factor is the welding speed which determines the keyhole size and consequently the evaporating surface area. It is therefore expected that volatile element losses decrease with increasing welding speed [9].

However, under the examined welding conditions (different welding speeds, 2m/min to 5 m/min and weld joint configurations), no significant changes in weld manganese concentration were found. This indicates that for the investigated welding parameters, this effect is not pronounced, allowing a stable welding process for the studied manganese alloyed stainless steels and avoiding considerable microstructural changes of the welded structures.

Pore formation by laser beam welding of the austenitic steels, as observed in the obtained welds, can be mainly linked to the penetration mode, joint configuration, sheet thickness and travel speed. Porosity tends to increase by welding in the overlap configuration at low welding speeds and when high penetration depths are reached. Laser beam welding in the overlap configuration is unfavourable, as it makes degassing of the vaporized material difficult. Depending on the resulting penetration depth, formed pores may not completely be expelled from the weld metal. Porosity can form due to gases released when high vapour pressure materials, like manganese and nitrogen are vaporized. The welding speed also influences pore formation, since it increases the keyhole stability, as reported in [13], where microfocused X-ray transmission investigations of the keyhole behaviour were carried out.

Another important aspect is that hot cracking occurred under conditions where pores were likely to form. In fact, there are some theories that suggest a connection between both phenomena. Dixon [10] postulated for example that cracks may be initiated at small gas bubbles which are entrapped between dendrites, based on real time radiographic observations. In [4, 5], models for hot cracking involving gas pore coalescence were presented.

It is also well known that solidification crack formation is linked to the tensile fracture of liquid films at grain boundaries within the mushy zone and that this is influenced by the interplay of metallurgical, thermal and mechanical factors. This will be discussed in detail below.

From the metallurgical standpoint, hot cracking is influenced by the alloy composition and impurity content. The beneficial effect of manganese in reducing hot cracking was for example reported in [12]. Though, this seems to contradict the fact that the alloy with the highest Mn content appears more susceptible to solidification crack formation. A possible explanation could be the existence of concentrated amounts of sulphur found in the form of precipitations (MnS) in the base material in combination with the phenomena occurring during laser beam welding. Evaporation of manganese, which is more intense in the keyhole [9], may favour the liberation of sulphur and hence the formation and accumulation of low melting phases in the weld centreline [17] at the last stages of solidification. The deleterious effect of sulphur is well known. The Fe-S eutectic may not only

lower the steel solidus temperature from 1400 to 988°C [6], but also contributes greatly to grain boundary wetting by a continuous liquid film, decreasing the resistance to cracking [1].
There is a relation between process parameters and encountered hot cracking, as well. Cracks only occurred at a high laser power (5kW). The heat input during welding affects the hot cracking behaviour significantly, primarily by affecting the amount and scale of segregation, but also by changing the thermo-mechanical conditions. Matsuda [14] showed for example that the resistance to hot crack formation decreases with increasing laser power and welding speed, as well as with narrower weld shape.
In general, high laser welding speeds and the resulting high cooling rates lead to the formation of a characteristic grain structure in which the solidified crystals adjoin in the middle of the weld. This is beneficial to the accumulation of low melting eutectic phases in the weld centre [18].
Considering the mechanical influencing factors, critical strain rates can be associated with crack formation, as proposed in [7, 16]. Strain rate is considered a key controlling factor for both crack initiation and growth.
In this regard, the CTW-Test was developed to measure and define the critical strain rate for different materials. The main advantage of this test lies in the possibility of varying the local strain rates which can be directly linked to a hot cracking mechanism.
CTW-Test results showed a higher hot cracking susceptibility of the manganese alloyed steel and let induce that the critical strain rate is in this case lower, in comparison to that of the standard CrNi-steel. Measurement of the local strain during the CTW-Test will follow in further investigations in order to establish a direct correlation between a critical strain rate and hot cracking. Preliminary performed CTW-Tests allowed only the measurement of the resulting crack length in dependence of the applied cross-head speed, but can quite well be used to rank the hot crack susceptibility of the investigated alloys. The results are furthermore consistent with those obtained from the conducted welding experiments.
It must also be mentioned that weldability rankings based upon other welding techniques (as presented in [11]) may not be transferable to laser welds and vice versa, due to the unique characteristics of the laser beam welding process. These include, for example, high temperature gradients and solidification rates that lead to high undercooling. In addition, the local strain distribution around rapidly moving laser welds is expected to react differently to global restraining forces.

Conclusions

Laser beam weldability of high-manganese alloyed stainless steels was found to be strongly parameter dependent. Spattering, porosity and hot crack formation are encountered phenomena that influence the weld quality, but were proved to be preventable by adequate parameter settings.
High quality butt welded joints could be produced at different welding parameters and sheet thicknesses. In overlap welding of 3.2 mm sheets, internal imperfections arose, but could however be avoided by adjusting the travel speed and laser power.
No significant decrease in manganese concentration was detected at the investigated welding parameters and conditions. The obtained weld microstructure is comparable with that of the base material.
The CTW-Test was used to examine the hot cracking susceptibility based on critical strain rates. The objective was to provide knowledge of the weldability of high manganese alloyed steels in comparison to standard grades and validate the results based on experimental data from produced butt and lap welds. Application of variable controlled tensile strain transverse to the welding direction contributes to crack formation, as it influences local strain rates experienced by the weld. Preliminary results showed an increased hot cracking susceptibility of the high manganese alloy steel, obtained from the measured total crack length in dependence of the applied cross-head speed, which is in accordance with experimental welding observations. A further aim is to quantify the critical strain rate required for hot crack formation by measuring the local strains in/near the mushy zone of the weld.

Acknowledgments

The authors would like to thank the Federation of Industrial Research Associations (AiF Arbeitsgemeinschaft industrieller Forschungsvereinigungen) and the German Federal Ministry for Trade, Industry and Technology (BMWi Bundesministerium für Wirtschaft und Technologie) for making this research possible by funding it in the Project 16208 N, “Laser beam welding of austenitic and austenitic-ferritic CrMnNi-steels”. Karin Schlechter, Karen Stelling, Nicolas Coniglio and Marina Marten greatly contributed to the experimental part of presented results.

Bibliographic references

[1] BORLAND, J.C. Generalized theory of super-solidus cracking in welds (and castings). ***British Welding Journal***, p. 508–512, 1960.

[2] BROOKS, J.A. Weldability of high N, high Mn austenitic stainless steel. ***Welding Research Supplement***, p. 189–195, 1975.

[3] CORTIE, M. B. Copper as an austenitizing addition to stainless steels. In: XVTH CMMI CONGRESS. 1994. V. 2, p. 165–172.

[4] CONIGLIO, N. Aluminum alloy weldability: Identification of weld solidification cracking mechanisms through novel experimental technique and model development. Fakultät für Maschinenbau der Otto-von-Guericke-Universität Madgeburg, 2008. 208p.

[5] CROSS, C.E. et al. The role of porosity in initiating weld metal hot cracks. In: AWS CONF. PROC. MODELLING AND CONTROL OF JOINING PROCESSES. 1994. p. 549–557.

[6] CROSS, C.E. On the origin of weld solidification cracking. In: ***Hot Cracking Phenomena in Welds***. Berlin: Springer, 2005. 394p. cap. 1, p. 3–18.

[7] CROSS, C.E. & CONIGLIO N. Weld solidification cracking: Critical conditions for crack initiation and growth. In: ***Hot Cracking Phenomena in Welds II***. Berlin Heidelberg: Springer, 2008. 467p. cap. 1, p. 39–57.

[8] CHARLES, J. The new 200-series: an alternative answer to Ni surcharge? Risks and opportunities. ***La Revue de Métallurgie – CIT***, p. 308–317, 2007.

[9] DILTHEY, U. al. Development of a theory for alloying element losses during laser beam welding. ***Journal of Physics D: Applied Physics***, p.34:81–86, 2001.

[10] DIXON, B.F. & Ritter, J.C. Real time radiographic study of weld metal solidification crack formation in steels. ***Metallurgical and Materials Transactions A***. March, 1991.

[11] HASE, S. et al. Schweißeignung kaltverformter nichtrostender austenitischer CrNi-Stähle. In: Die Verbindungs Spezialisten 2008. Dresden. 2008. p. 168–173.

[12] HONEYCOMBE, J. & GOOCH, T.G. Effect of manganese on cracking and corrosion behaviour of fully austenitic stainless-steel weld-metals. ***Metal Construction and British Welding Journal***, v. 4, n.12, p. 456–460, 1972.

[13] KATAYAMA, S. Fundamentals of Fiber Laser Welding. In: INTERNATIONAL COLLOQUIUM HIGH POWER LASER WELDING, 2009. Berlin.

[14] KHAN, P.A.A. et al. Laser beam welding of high-manganese stainless steels - Examination of alloying element loss and microstructural changes. *Welding research supplement*, p. 1–7, 1988.

[14] MATSUDA, F., NAKAGAWA, K. Solidification crack susceptibility in laser beam weld metal of 0.2C-low alloy steels. *Transactions of JWRI*, v. 16, p. 130–114, 1987.

[15] MYSLOWICKI, S. Das Auscheidungs- und Korrosionsverhalten eines stickstofflegierten, austenitischen Chrom-Nickel-Stahls mit abgesenktem Nickelgehalt. Shaker Verlag, 2007. 136p.

[16] RAPPAZ, M. et al. A new hot-tearing model. ***Met Mat Trans 30A***, .p. 449-455, 1999.

[17] SAVAGE, W.F. & ARONSON, A.H. Preferred orientation in the weld fusion zone. ***Welding Journal***, v. 45, p. 85–89, 1966.

[18] SAVAGE, W.F. et al. Segregation and hot cracking in low-alloy quench and tempered steels. ***Welding Journal***, v. 47, p. 420–425, 1968.

[19] SUUTALA, N. Effect of manganese and nitrogen on the solidification mode in austenitic stainless steel welds. ***Metallurgical Transactions A***, v. 13 A, p. 2121–2130, 1982.
[20] TOOR, I. et al. Development of high Mn-N duplex stainless steel for automobile structural components. ***Corrosion Science***, v. 50, p. 404–410, 2008.
[21] ZHAO, L. et al. Microstructure and mechanical properties of heat-affected zone of high nitrogen steel simulated for laser welding conditions. ***ISIJ International***, 47, p. 1351–1356, 2007.

Corresponding author:
Vanessa Quiroz
Vanessa.Quiroz@bam.de
BAM Federal Institute for Materials Research and Testing, Berlin, Germany
Division V.5 "Safety of Joined Components"
Unter den Eichen 87
12205 Berlin